Cell, Vol. 106, 331–341, August 10, 2001, Copyright ©2001 by Cell Press

Structure of Bovine Mitochondrial F_1-ATPase with Nucleotide Bound to All Three Catalytic Sites: Implications for the Mechanism of Rotary Catalysis

R. Ian Menz,[1,4] John E. Walker,[1,2,3] and Andrew G.W. Leslie[1,3]

[1] Medical Research Council Laboratory of Molecular Biology
Hills Road
Cambridge CB2 2QH
United Kingdom

[2] Medical Research Council Dunn Human Nutrition Unit
Hills Road
Cambridge CB2 2XY
United Kingdom

Summary

The crystal structure of a novel aluminium fluoride inhibited form of bovine mitochondrial F_1-ATPase has been determined at 2 Å resolution. In contrast to all previously determined structures of the bovine enzyme, all three catalytic sites are occupied by nucleotide. The subunit that did not bind nucleotide in previous structures binds ADP and sulfate (mimicking phosphate), and adopts a "half-closed" conformation. This structure probably represents the posthydrolysis, pre-product release step on the catalytic pathway. A catalytic scheme for hydrolysis (and synthesis) at physiological rates and a mechanism for the ATP-driven rotation of the γ subunit are proposed based on the crystal structures of the bovine enzyme.

Introduction

F_1-ATPase is the water soluble component of ATP synthase (F_1F_o-ATPase), the enzyme responsible for the synthesis of ATP from ADP and Pi using energy derived from the transmembrane proton motive force (Boyer, 1997; Deckers-Hebestreit and Altendorf, 1996; Walker, 1998; Weber and Senior, 1997). When separated from the intact enzyme, the F_1 component (subunit stoichiometry $\alpha_3\beta_3\gamma_1\delta_1\epsilon_1$) hydrolyzes ATP. Both ATP synthase and F_1-ATPase display remarkable cooperativity between the three catalytic sites, which are in the β subunits at the interfaces with the α subunits. According to the binding change mechanism of catalysis (Boyer, 1993), the three catalytic sites are in different conformations at any given time, but interconvert sequentially between these different conformations as catalysis proceeds. The mechanism is supported by biochemical and kinetic data (reviewed in Boyer, 1993) and by the crystal structure of the bovine mitochondrial F_1-ATPase (Abrahams et al., 1994), which showed a marked asymmetry in the conformations and nucleotide occupancy of the β subunits. Features of this structure suggested that the interconversion between the different conformations of the β subunits was achieved by rotation of the central γ subunit relative to the $(\alpha\beta)_3$ subcomplex. Experimental evidence for rotation in F_1-ATPase has been obtained from crosslinking (Duncan et al., 1995) and spectroscopic studies (Sabbert et al., 1996), and by direct visualization of fluorescently labeled actin filaments attached to the γ subunit (Noji et al., 1997).

Tryptophan fluoresence has been used to monitor nucleotide binding to the catalytic sites in an engineered mutant (βTyr331 →Trp) of the enzyme from *Escherichia coli* (Weber and Senior, 1997). Parallel measurements of nucleotide binding and catalysis as a function of ATP concentration suggested that maximum rates of hydrolysis are achieved only when (on average) all three catalytic sites are occupied (Weber et al., 1993). By contrast, the classical binding change mechanism (Boyer, 1993) is generally presented as having at most two of the three catalytic sites occupied by nucleotide (Fersht, 1998; Stryer, 1995).

This paper describes the crystal structure of an aluminium fluoride inhibited form of bovine mitochondrial F_1-ATPase in which nucleotide is bound to all three catalytic subunits. This structure displays a novel conformation which is believed to represent an important intermediate on the catalytic pathway. Comparison with previous structures provides an insight into catalytic cooperativity, and suggests a possible mechanism for the generation of rotation of the γ subunit.

Results and Discussion

Bovine mitochondrial F_1-ATPase was inhibited by treatment with aluminium fluoride as described previously (Braig et al., 2000), and the inhibited enzyme was crystallized in the presence of aluminium fluoride and MgADP (see Experimental Procedures). The structure was solved by molecular replacement and refined against X-ray data to 2.0 Å resolution (Table 1). The resulting structure is the most detailed currently available for this complex oligomeric assembly, revealing, for example, the complete coordination of the magnesium ions at the nucleotide binding sites for the first time. As previously observed in the structure of F_1-ATPase inhibited with dicyclohexylcarbodiimide (F_1-DCCD) (Gibbons et al., 2000), the smaller unit cell (compared to that of the original structure) results in improved ordering of the central stalk, which is made up of the γ, δ, and ϵ subunits.

Comparison with the structure of the previously determined aluminium fluoride complex (Braig et al., 2000) reveals two novel features. First, MgADP-fluoroaluminate is bound at two catalytic sites rather than one. This stoichiometry is consistent with previous biochemical studies (Dou et al., 1997; Issartel et al., 1991; Nadanaciva et al., 2000). Second, the third catalytic subunit (β_E), that has no bound nucleotide in all previously determined structures of bovine F_1-ATPase, binds ADP and what is

[3] Correspondence: andrew@mrc-lmb.cam.ac.uk (A.L.), jew@mrc-dunn.cam.ac.uk (J.W.)

[4] Present address: Department of Biochemistry, University of Sydney, New South Wales 2006, Australia.

Table 1. Data Processing and Refinement Statistics for Bovine $(ADP.AlF_4^-)_2F_1$-ATPase

Resolution (Å)	13.5–2.0
Number of reflections	209,953
Multiplicity[a]	2.1 (1.5)
Completeness[a,b] (%)	79.6 (40.6)
R_{merge}[a] (%)	6.6 (48.1)
$<I/\sigma(I)>$[a]	9.1 (1.8)
B factor from Wilson plot ($Å^2$)	26.7
Refinement	
Number of reflections	200,363
Total number of atoms	26,329
Number of waters	1,693
R factor (%)	20.1
R_{free}[c] (%)	26.4
Rms deviation in bond lengths (Å)	0.012
Rms deviation in bond angles (°)	1.1

[a] The value for the highest resolution bin (2.14–2.00 Å) is given in parentheses.
[b] The completeness is 95% to 2.3 Å. The completeness at 2 Å is low because this data was only recorded in the corners of the detector.
[c] The R_{free} was calculated for 9590 randomly chosen reflections which were excluded from the refinement.

assumed to be a sulfate ion (see Experimental Procedures and Figure 1a), so that all three catalytic sites are occupied. Nucleotide binding to the β_E subunit is accompanied by a large conformational change in that subunit, and smaller changes in the adjacent α_E and β_{DP} subunits.

Quaternary and Tertiary Structural Changes in F_1-ATPase

The original F_1-ATPase structure, which will be referred to as "native," was determined using crystals grown in the presence of AMP-PNP and ADP (Abrahams et al., 1994). The first crystals of the aluminium-fluoride inhibited enzyme, $(ADP.AlF_3)F_1$, were grown under similar conditions (Braig et al., 2000). The current structure, determined from crystals grown in the presence of ADP and fluoroaluminate, has two catalytic sites occupied by ADP-fluoroaluminate, and will be referred to as $(ADP.AlF_4^-)_2F_1$. All noncatalytic subunits bind ADP.

Comparison of the different conformational states of F_1-ATPase is simplified by defining a frame of reference that is common to all structures. The six N-terminal domains of the $(\alpha\beta)_3$ subassembly appear to form a stable crown to the structure, which serves as a natural point of reference. Changes in quaternary and tertiary structure can be demonstrated by examining the rms differences (rmsd) in α-carbon positions for each domain after superimposing all six corresponding N-terminal domains. The results of these comparisons for the native and $(ADP.AlF_4^-)_2F_1$ structures are given in Table 2. The rmsd values when the domains are superimposed individually gives an estimate of the conformational changes within each domain. As expected, the N-terminal domains show very little variation. The magnitude of these differences probably reflects the level of coordinate error for well-ordered regions of the models. The nucleotide binding domains show slightly larger movements but, with the notable exception of the β_E subunit, these domains superimpose quite well. The small differences obtained when comparing these subunits individually demonstrate that, with the exception of the β_E subunit, there is no significant conformational change within the nucleotide binding domains. The much larger rmsd for the β_E subunit is the result of a rotation of the lower part of this domain, which moves together with the C-terminal domain as discussed below. The C-terminal domains show the largest differences. In the α_{TP}, α_{DP}, and β_{TP} subunits, these reflect partly the higher mobility of this domain (as shown by the larger average temperature factors), but significant differences are found between the α_E, β_{DP}, and β_E subunits. Of these, the most dramatic results from a 16° rotation of the C-terminal domain in the β_E subunit, which is associated with binding ADP and sulfate in the $(ADP.AlF_4^-)_2F_1$ structure. This rotation has the effect of closing the interface between the α_E and β_E subunits, partially burying the bound nucleotide (Figures 1b and 1c). The relatively small rotation (3°) of the same domain in the α_E subunit also contributes to the closure of this catalytic interface. The change in tertiary structure of the α_E subunit affects the adjacent β_{DP} subunit, where there is an even smaller (1.3°) rotation of the C-terminal domain. Nucleotide binding to the β_E subunit results in significant shifts in the β_E, α_E, and β_{DP} subunits, but very little change in the α_{TP} subunit, despite the extensive interface between the β_E and α_{TP} subunits. It is probable that this asymmetry plays an important role in the binding change mechanism of catalysis, where binding of substrates to one β subunit promotes catalysis at a second β subunit.

Conformational States of the Catalytic β Subunits

On the basis of the native F_1-ATPase and the $(ADP.AlF_4^-)_2F_1$ structures, it is possible to define three distinct conformations for the catalytic β subunits. These conformations can be described as "closed," with high affinity for nucleotide, "half-closed," with intermediate affinity, and "open," with low affinity. They are described in detail below.

The β_{TP} and β_{DP} subunits in $(ADP.AlF_4^-)_2F_1$ adopt very similar closed conformations. Individual domains superimpose with rmsd values of 0.16 Å and 0.38 Å for α-carbon positions in the N-terminal and nucleotide binding domains. In the C-terminal domain, the rmsd is larger (0.92 Å), but this is due to large deviations (up to 3 Å) for residues β384–400. This region interacts with the γ subunit, and the differences are a consequence of the asymmetric association of the γ subunit with the $(\alpha\beta)_3$ subassembly. If these residues are excluded, the rmsd drops to 0.29 Å. The entire β subunit superimposes with an rmsd of 0.72 Å. This value is larger than those for individual domains, and results from a small (2°) rotation of the N- and C-terminal domains relative to the nucleotide binding domain. These small rotations have no significant effect on the positions of residues in the immediate vicinity of the nucleotide binding site.

The nucleotide-free β_E subunit in the native structure represents the low affinity or open state. If the N-terminal domains of the β_{DP} and β_E subunits in this structure are superimposed, then the C-terminal domains are related by a rotation of 33°. Residues β132–173 and β330–364, which form the lower three strands (3, 8, and 9) of the

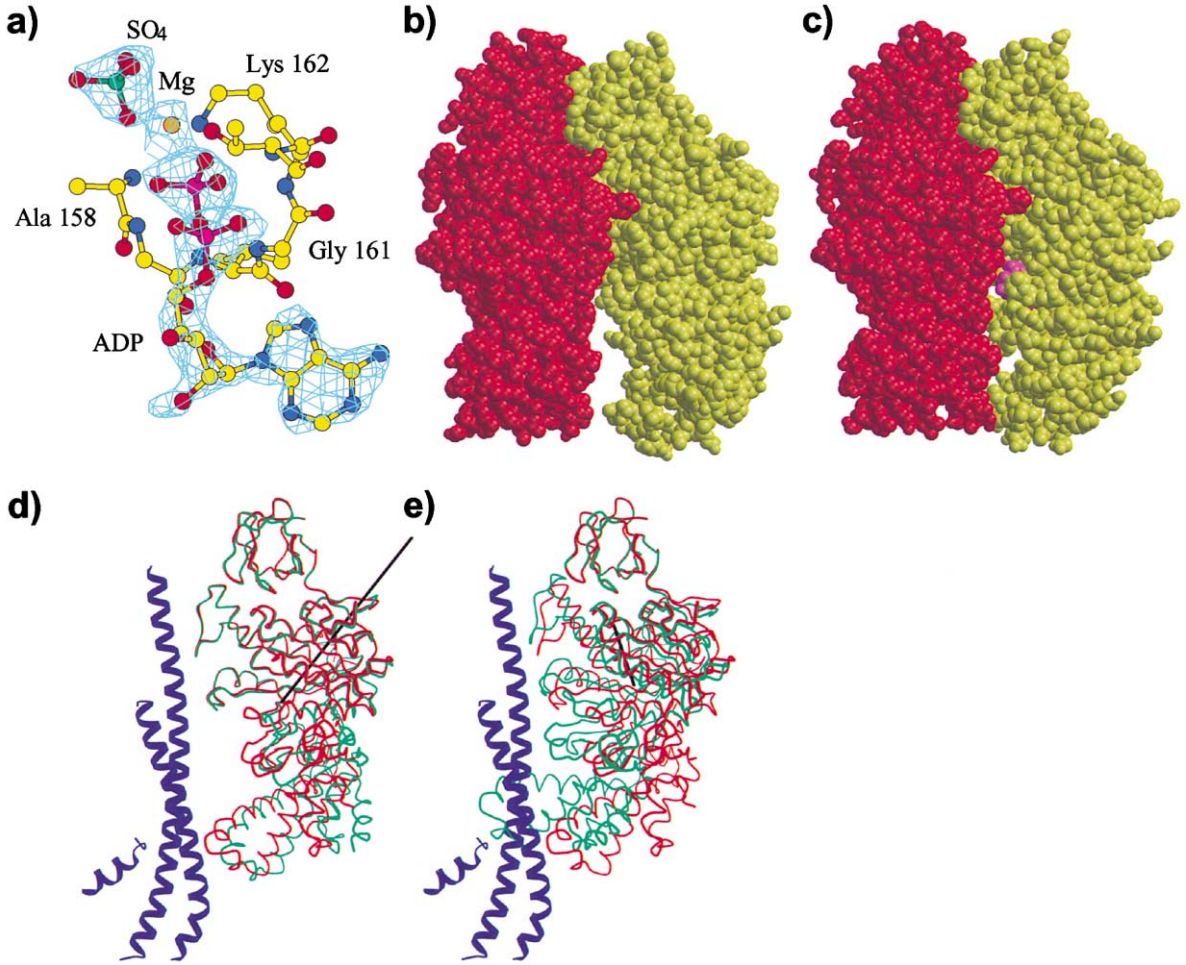

Figure 1. Conformational Changes due to Nucleotide Binding in the β_E Subunit of Bovine F_1-ATPase

(a) Difference electron density for ADP, sulfate, and magnesium bound to the β_E subunit of $(ADP.AlF_4^-)_2F_1$. The electron density was calculated with model phases before inclusion of ADP, Mg, or SO_4 in the model. Contours are drawn at 3σ. Parts (b) and (c) show space filling representations of the α_E (red) and β_E (yellow) subunits in the native structure (b) and the $(ADP.AlF_4^-)_2F_1$ structure (c). In (c), the nucleotide is shown in magenta. (d) Ribbon representation of the β_{ADP+Pi} subunit (red) superimposed on the β_E subunit (green) of the native structure and (e) on the β_{DP} subunit (green) of the $(ADP.AlF_4^-)_2F_1$ structure. The γ subunit of the $(ADP.AlF_4^-)_2F_1$ structure is shown in blue. For clarity, the γ subunit of the native structure is not shown. The rotation axis that relates the two conformations of the lower region of the nucleotide binding domains and C-terminal domains is drawn in black.

β sheet in the nucleotide binding domain and their associated α helices (B, H, and I), rotate together with the C-terminal domain (β365–478) as a single, approximately rigid, group. The rotation axis lies close to the plane of the β sheet, in a direction at almost 90° to the β strands. There are significant changes (>30°) in backbone torsion angles in many different regions of the nucleotide binding domain, but the largest changes (>100°) occur in the loop linking helix B to β strand 4 (β176–180). Mutagenesis of glycine residues in this loop in F_1-ATPase from the thermophilic *Bacillus* PS3 results in a dramatic loss of activity (Masaike et al., 2000), confirming that backbone flexibility of this region is essential for catalysis.

In the $(ADP.AlF_4^-)_2F_1$ structure, the β_E subunit binds ADP and sulfate and adopts the half-closed conformation (β_{ADP+Pi}) that is intermediate between the closed and open states. The C-terminal domain of the β_{ADP+Pi} subunit is related to the open conformation by a rotation of 16°, and to the closed conformation by a rotation of 23° (Figures 1d and 1e). However, the directions of these two rotation axes are almost orthogonal. The 16° rotation is approximately around the axis of the $(\alpha\beta)_3$ subcomplex and has the effect of closing the α_E/β_E catalytic interface (Figure 1c). The larger rotation is about an axis approximately orthogonal to the particle axis and results in the correct placement of the catalytic residues βGlu188, βArg189 relative to the phosphate groups of the nucleotide. In both of these structural transitions, residues β132–173, β330–364, and the C-terminal domain (β365–478) move approximately as a rigid group. The only significant exception to this is the loop formed by residues β421–427, part of the adenine binding pocket, which is disordered in the native β_E subunit.

Comparison of the Catalytic Sites

The catalytic site of the β_{DP} subunit in the $(ADP.AlF_4^-)_2F_1$ structure is shown in Figure 2a. The geometry of fluoro-

Table 2. Conformational Differences between the Structures of Native and $(ADP.AlF_4^-)_2F_1$-ATPase

Domain	Subunit					
	α_{TP}	α_{DP}	α_E	β_{TP}	β_{DP}	β_E
N-terminal	0.33	0.27	0.21	0.21	0.27	0.26
α24–91, β10–81	(0.31)	(0.24)	(0.20)	(0.20)	(0.26)	(0.22)
<B> Å^2	38.1	35.5	35.9	34.5	35.2	37.8
Nucleotide binding	0.39	0.35	0.45	0.40	0.59	2.12
α96–379, β83–363	(0.32)	(0.24)	(0.28)	(0.26)	(0.29)	(1.44)
<B> Å^2	34.6	31.8	33.3	34.8	34.3	47.1
C-terminal	0.56	0.71	1.11	0.78	1.32	6.72
α380–510, β364–474	(0.49)	(0.33)	(0.56)	(0.44)	(0.57)	(1.05)
<B> Å^2	59.3	37.8	43.3	46.6	39.0	82.4

Rms differences in α-carbon positions in the native and $(ADP.AlF_4^-)_2F_1$ following superposition of the six N-terminal domains. The values in parentheses are the rms differences when individual domains are superimposed. The mean temperature factor is for main chain atoms in the $(ADP.AlF_4^-)_2F_1$ structure. The native coordinates were those of the structure determined at 100 K (PDB accession code 1e1q) (Braig et al., 2000).

aluminate binding is very similar to that found in the β_{DP} subunit of the $(ADP.AlF_3)F_1$ structure (Braig et al., 2000) (Figures 2b and 2c) in spite of the fact that AlF_4^- is bound rather than AlF_3. The most significant difference is in the distances between the aluminium and its apical ligands, which are shorter in the present structure and much closer to the values found in other NDP.AlF_x-inhibited hydrolases. The coordination of the AlF_4^- group reaffirms the likely importance of two arginine residues (αArg373 from the neighboring α subunit and βArg189) and the P loop lysine (βLys162) in providing charge stabilization of a putative pentacoordinate transition state. The carboxylate group of βGlu188 coordinates a water molecule which is an apical ligand to the Al^{3+} ion, consistent with a role for this residue in polarizing or deprotonating a water molecule for inline attack on the γ-phosphorous group in the hydrolytic reaction. The Mg^{2+} ion is coordinated by a β-phosphate oxygen (2.1 Å), a fluorine ion (1.9 Å), the hydroxyl of the P loop βThr163 (2.1 Å), and three water molecules (1.9 Å, 2.2 Å, and 2.3 Å). Two of these waters form hydrogen bonds with the carboxylate oxygens of βGlu192, while the third hydrogen bonds to a carboxylate oxygen of βAsp256 (in the Walker B motif). By analogy with other AlF_x-inhibited NTPases, this active site conformation can be interpreted as modeling a transition state of the reaction. Site-directed mutagenesis of residues equivalent to βLys162, βGlu188, βArg189, βAsp256, and αArg373 in *E. coli* F_1-ATPase supports the proposed roles for these residues in catalysis (Amano et al., 1996; Lobau et al., 1997; Nadanaciva et al., 1999a, 1999b), although the precise role of αArg373 is contentious (Le et al., 2000).

Although the conformation of the β_{TP} subunit is very similar to that of the β_{DP} subunit, the catalytic sites are not equivalent, due to the different relative positions of the corresponding α subunits (which contribute residues to the catalytic sites). The β_{TP} catalytic site is more open than that of the β_{DP} subunit (Figure 3a). In particular, the guanidinium group of αArg373 is over 1 Å further from the γ-phosphate position in the β_{TP} catalytic site (Figure 3b). The other catalytic residues (βLys162, βGlu188, βArg189) have moved by between 0.3 Å and 0.6 Å. Although these differences are relatively small, they could have a marked effect on catalysis. Site-directed mutagenesis of F_1-ATPase from *Bacillus* PS3 has shown that mutation of the catalytic glutamate to aspartate, resulting in a movement of the carboxylate group by about 1.5 Å, results in a reduction in activity to 7% of wild-type (Amano et al., 1994). When assigning the probable catalytic state of a site, it is therefore important to distinguish between the conformation of the site, consisting of the relevant β/α heterodimer, and the conformation of the catalytic β subunit.

The half-closed conformation found in the β_{ADP+Pi} subunit of the $(ADP.AlF_4^-)_2F_1$ structure is likely to represent the posthydrolysis product state of the reaction, with the sulfate group mimicking the cleaved γ-phosphate. The positions of residues involved in binding the nucleotide, including βVal164, βTyr345, βPhe418, and βPhe424, which form the adenine and ribose binding pocket, and the P loop residues (β159 and β161–163) which interact with the α- and β-phosphates, are essentially unchanged relative to the closed conformation (Figure 3c). However, the side chains of the catalytic residues βGlu188, βArg189, and αArg373 have moved 6.5 Å, 3.9 Å, and 4.1 Å, respectively. These shifts are a result of the 23° rotation of the lower part of the nucleotide binding domain and the C-terminal domain and in addition to a large change in the main chain torsion angles of βGlu188 (−110°,−155° (β_{DP}) to −65°,130° (β_{ADP+Pi})). The carboxylate group of βGlu188 now stacks against the side chain of βTyr219, and is remote from the active site. The sulfate group lies 3.5 Å away from the position of the AlF_4^- group in the closed conformation and is coordinated by the guanidinium groups of αArg373 (3.0 Å) and βArg189 (2.9 Å) and the ε-amino group of βLys162 (2.9 Å). The phosphate binding site is only present in the half-closed conformation of the β_{ADP+Pi} subunit. In both the closed and open conformations, the relative positions of these three side chains (αArg373, βLys162, and βArg189) are very different (Figures 3c and 3d), and in the former, the phosphate site is occupied by the side chain of βTyr311. Assuming that the half-closed conformation is transient in nature and only occurs during catalysis, this is consistent with the very low affinity of Pi for soluble F_1-ATPase ($K_d(Pi) > 10$ mM for the *E. coli* enzyme; Weber and Senior, 1997).

The low nucleotide affinity of the β_E subunit of the native structure can be explained by comparing it to the β_{ADP+Pi} subunit in $(ADP.AlF_4^-)_2F_1$ (Figure 3d). Firstly, the

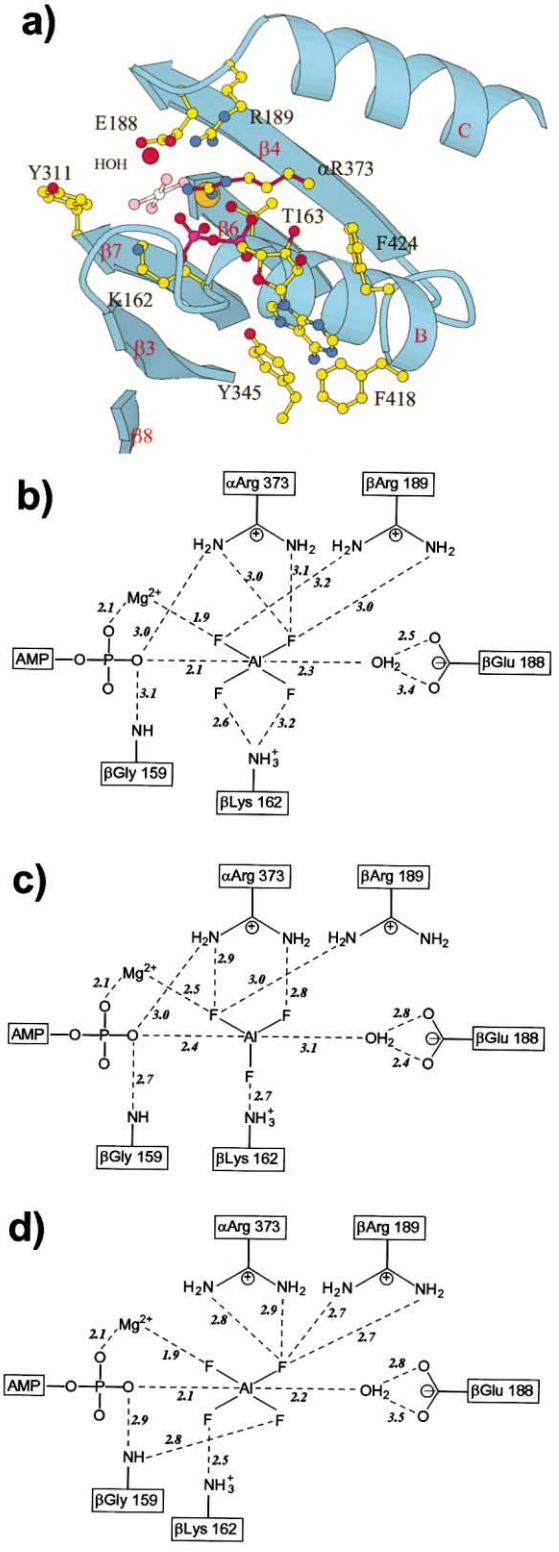

Figure 2. The Coordination of Aluminium Fluoride in the Catalytic Sites of Bovine F_1-ATPase

(a) Residues involved in nucleotide binding and catalysis and the elements of secondary structure in the β_{DP} subunit of the (ADP.AlF_4^-)$_2F_1$ structure. Atom colors are yellow (carbon), blue (nitrogen), red (oxygen), pink (fluoride), magenta (phosphorous), orange (magnesium), and gray (aluminium). (b–d) Schematic representations of the coordination of the aluminium fluoride group bound to the catalytic sites of (b) the β_{DP} subunit of the (ADP.AlF_4^-)$_2F_1$ structure, (c) the β_{DP} subunit of the (ADP.AlF_3)F_1 structure, and (d) the β_{TP} subunit of the (ADP.AlF_4^-)$_2F_1$ structure. Possible hydrogen bond interactions are shown as dotted lines. All distances are in Å.

residues in the P loop (β156–163) are less well ordered (mean B 74 Å^2 compared to 39 Å^2 in the β_{ADP+Pi} subunit) and there are changes in main chain conformation. Secondly, the adenine binding pocket is highly distorted. The side chain of βPhe424 has moved by 4 Å, and the loop containing this residue (β421–428) is very mobile (B >100 Å^2 for main chain atoms). The side chain of βTyr345 has also moved by 2 Å, and the large relative movement of the adjacent α_E subunit results in the entire nucleotide binding site becoming solvent accessible. Thirdly, the side chain of βLys162, which interacts with the nucleotide phosphate groups when nucleotide is bound, adopts an extended conformation and forms a salt-bridge with βAsp256. Fourthly, the Mg^{2+} binding site is disrupted by a change in the orientation of the side chain of βThr163, displacing the hydroxyl that normally coordinates Mg^{2+}. In addition, the new interaction between βLys162 and βAsp256 disrupts the interaction between the latter residue and Mg^{2+} via a bridging water seen in the nucleotide binding subunits. Finally, catalytically important residues such as βGlu188, βArg189, and αArg373 have moved significantly. The structural rearrangement accompanying conversion of the open to the half-closed conformation is a striking example of induced fit.

The Binding Change Mechanism of Catalysis

According to the binding change mechanism of catalysis (Boyer, 1993), each catalytic site alternates sequentially between three different states: the tight state (where catalysis occurs), the loose state (where substrates are bound), and the open state (with low affinity for nucleotide).

The conformation of the catalytic site found in the β_{DP} subunits of the (ADP.AlF_4^-)$_2F_1$ and native structures provides the best model for the tight state. This site was thought to represent the tight state in the native structure for two reasons. First, the presence of bound MgADP was consistent with the enzyme being in the MgADP inhibited form, in which MgADP (but no phosphate) is bound to the catalytic site with the highest nucleotide affinity (reviewed in Boyer, 1997). Second, the catalytic interface is more buried for the β_{DP} subunit than for the β_{TP} subunit, consistent with the need to exclude bulk solvent. Subsequently, the presence of MgADP.AlF_3 in the β_{DP} subunit of the aluminium fluoride inhibited structure (Braig et al., 2000) also suggested that this subunit is in the catalytically active conformation. In the (ADP.AlF_4^-)$_2F_1$ structure, the geometry of the active site residues is very similar in the β_{DP} and β_{TP} subunits (Figure 3b). However, the increased proximity of the guanidinium group of αArg373 to the AlF_4^- group in the β_{DP} subunit suggests that this represents the catalytic conformation. On this basis, the more open site on the β_{TP} subunit would correspond to the loose state, and the β_E subunit corresponds to the open state.

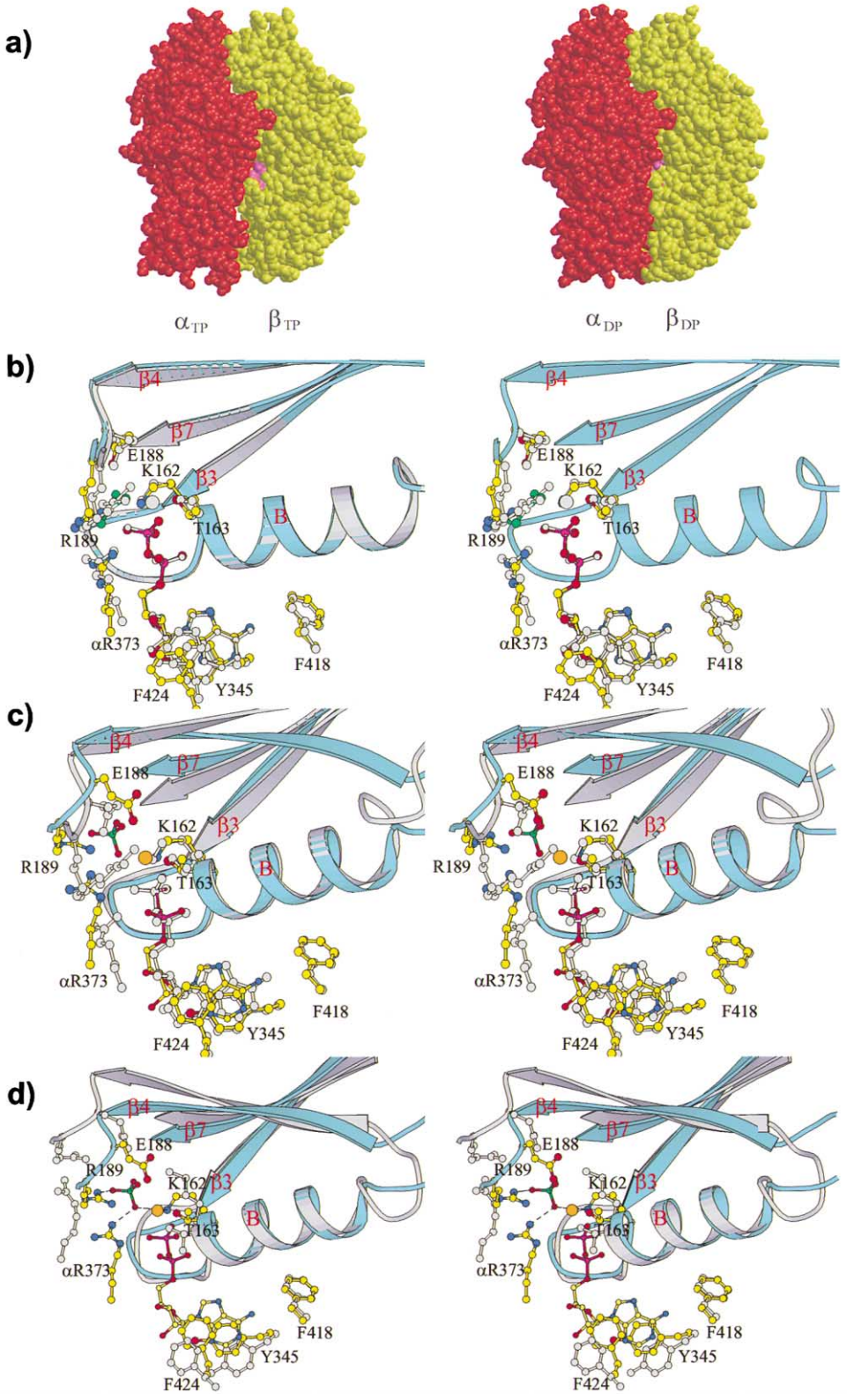

Figure 3. Comparison of the Catalytic Sites in Bovine F_1-ATPase

(a) Space filling representations of the catalytic interface of the β_{TP} and β_{DP} subunits in the $(ADP.AlF_4^-)_2F_1$ structure. The α subunits are shown in red, the β subunits in yellow, and the bound nucleotide in magenta. (b–d) Stereo views of the residues involved in nucleotide binding and catalysis and the elements of secondary structure in this region following superposition of residues β152–172.

(b) Comparison of the β_{TP} site (drawn with colored atoms and bonds and blue main chain ribbon) and the β_{DP} site (gray atoms, bonds, and main chain).

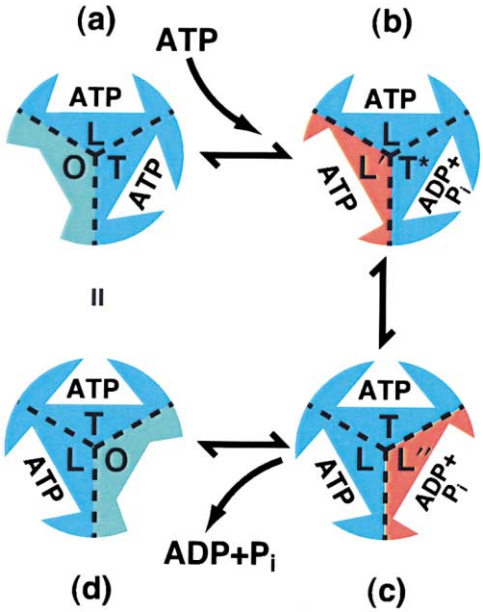

Figure 4. A Scheme for the Binding Change Mechanism of Catalysis in F_1-ATPase at Saturating Concentrations of ATP Based on the Bovine Crystal Structures

The present structure is thought to represent a novel intermediate on the catalytic pathway of F_1-ATPase. Significantly, it demonstrates that there is an asymmetric state in which all three β subunits bind nucleotide, but only two β subunits adopt a closed conformation. Cross-linking experiments with the thermophilic F_1-ATPase suggest the existence of such a conformation on the catalytic pathway (Tsunoda et al., 1999). With the assumption that the open (nucleotide free) conformation of the β subunit is relatively short lived when the substrate concentration is high enough to ensure maximum turnover, the structure is also consistent with tryptophan fluorescence studies, which show that, on average, all three catalytic sites are occupied under these conditions (Weber et al., 1993). Based on crystal structures of bovine F_1-ATPase, a catalytic scheme for ATP hydrolysis in F_1 under conditions of high substrate concentration has been devised (Figure 4). ATP binding to the open catalytic site (O) produces a conformational change to a half-closed state (L′), which has not yet been observed crystallographically but is probably similar to the β_{ADP+Pi} conformation. Conformational changes induced by ATP binding result in the committed hydrolysis of ATP at an adjacent catalytic site (T*), and cyclic interconversion of the sites. The T* site becomes a half-open site (L′′), the L site becomes a T site, and the L′ site becomes an L site. The existence of states corresponding to L′ and L′′ with preferential affinities for ATP and ADP have been suggested previously (Boyer, 2000). The crystal structure of $(ADP.AlF_3)F_1$, which has AMPPNP bound to the β_{TP} subunit and $MgADP.AlF_3$ bound to the β_{DP} subunit, provides the best structural model for the state shown in Figure 4a, although the original native structure is very similar. The $(ADP.AlF_4^-)_2F_1$ crystal structure described in this paper provides a satisfactory model for the state shown in Figure 4c. A crystal structure corresponding to Figure 4b has yet to be determined. The sequence of states for a single catalytic subunit (and the corresponding subunit conformation found in the crystal structures) is: $O(\beta_E) \rightarrow L'(\sim\beta_{ADP+Pi}) \rightarrow L(\beta_{TP}) \rightarrow T(\beta_{DP}) \rightarrow T^*(\beta_{DP}(ADP.AlF_4^-)_2) \rightarrow L''(\beta_{ADP+Pi}) \rightarrow O(\beta_E)$. Similar catalytic schemes have been proposed by Senior (Weber and Senior, 2000) and Allison (Ren and Allison, 2000). However, based on additional tryptophan fluorescence data (Weber et al., 1996), Senior has suggested that, on average, the enzyme binds two molecules of ADP and one molecule of ATP, rather than one molecule of ADP and two of ATP as shown in Figure 4. The Allison model has the same nucleotide occupancy as our proposed scheme, but it was suggested that catalysis occurs as the tight subunit is converted to an open conformation. This does not agree with the structural evidence, which suggests that the conformation of the transition state (MgADP and AlF_x bound) is essentially the same as the fully closed conformation; the opening of the subunit occurs after ATP hydrolysis rather than being required for formation of a transition state complex.

ATP Synthesis

Although the catalytic scheme shown in Figure 4 refers to ATP hydrolysis in F_1-ATPase, it is likely that ATP synthesis in ATP synthase follows a very similar sequence of steps but in reverse. In particular, the β_{ADP+Pi} subunit conformation would correspond to the Michaelis complex of the two substrates rather than the products of catalysis. In ATP synthase, a large increase in affinity for Pi is observed in the presence of a proton gradient (El-Shawi et al., 1990; Feldman and Sigman, 1983; Rosing et al., 1977). It has been suggested (Boyer, 2000) that rotation of the γ subunit, driven by proton translocation, is necessary for competent binding of ADP and Pi. The current structure provides support for this idea, as the phosphate binding site is only formed in the half-closed conformation of the β subunit, and rotation of the γ subunit is required to convert a β subunit from an open to a half-closed conformation. The arrangement of residues at the catalytic site of the β_{ADP+Pi} subunit also suggests how the enzyme selects the appropriate ligands for catalysis. In vivo, synthesis of ATP depends on binding ADP+Pi to the open β subunit in the presence of a large molar excess of ATP. Model building shows that it is not possible to accommodate an ATP molecule bound to the β_{ADP+Pi} subunit because of steric hindrance between the γ-phosphate and the guanidinium group of αArg373. This arginine residue may therefore fulfil multiple roles in catalysis, both stabilizing the pentacovalent transition state and acting as

(c and d) The β_{ADP+Pi} subunit (drawn with colored atoms and bonds and blue main chain ribbon) is shown superposed on (c) the closed conformation of the β_{DP} subunit (gray atoms, bonds, and main chain) and (d) the open conformation of the β_E subunit (gray atoms, bonds, and main chain). The P loop lies between the C-terminal end of β strand 3 and the α helix B. Hydrogen bonds to the sulfate group are drawn as dotted lines in (d). Atom colors as in Figure 2a, and green (sulfur).

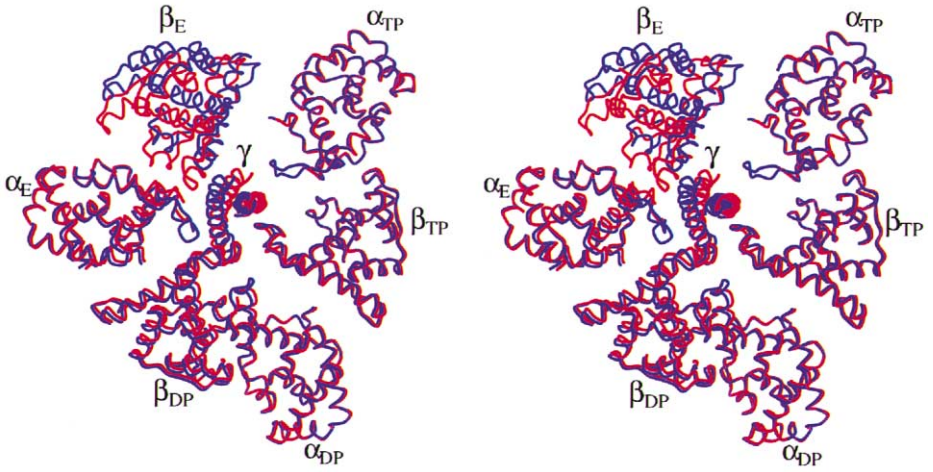

Figure 5. Rotation of the γ Subunit in Bovine F_1-ATPase

Stereo view of part of the γ subunit (residues 3–35 and 221–250) and the C-terminal domains of the $(\alpha\beta)_3$ hexamer in the native structure (blue) and the $(ADP.AlF_4^-)_2F_1$ structure (red), following superposition of the N-terminal domains. The β_E subunit shows the largest conformational change, but the rotation of the γ subunit is also apparent. Note that interacting residues in the β_E subunit and the γ subunit move in opposite directions.

a discriminator to ensure that the appropriate substrates are bound. By extension, it may also ensure that ATP (rather than ADP+Pi) is released from the catalytic site when it opens during ATP synthesis, and similarly that ADP+Pi are released during hydrolysis.

Rotation of the γ Subunit

Following superposition of the N-terminal domain crown in the native and $(ADP.AlF_4^-)_2F_1$ structures, the C-terminal residues (259–272) of the γ subunit, which lie in the sleeve of the bearing within the $(\alpha\beta)_3$ complex, superimpose well. However, the coiled-coil region has moved significantly (Figure 5), resulting in an overall rmsd of 2.9 Å in α-carbon positions for the entire γ subunit. The two conformations of the γ subunit are related by a rotation that varies in magnitude along the length of the C-terminal helix, ranging from less than 1° for the final residues (γ259–272) to a maximum of about 20° for residues γ234–244 (which form the coiled-coil with residues γ20–10). The axis for the rotation is almost parallel to and coincident with the axis of pseudosymmetry of the $(\alpha\beta)_3$ subassembly, so that the observed rotation, although small, is probably similar to the rotation that occurs during catalysis. The variation in the rotation angle implies that the coiled-coil is slightly more twisted in the $(ADP.AlF_4^-)_2F_1$ structure than in the native form.

Assuming that the current structure represents the posthydrolysis, pre-product release state, the next step on the catalytic cycle will be product release (β_E subunit in the fully open conformation), followed by substrate (ATP) binding to the β_E subunit. This latter step probably results in a partially closed conformation of the β_E subunit similar to that observed in the current structure. On this basis, the rotation of the γ subunit during the product release and substrate binding steps is likely to be quite small and not uniform over the length of the γ subunit. The greater part of the 120° rotation that accompanies a single catalytic turnover will be associated with the committed ATP hydrolysis step.

The 120° rotation has recently been resolved into two substeps of approximately 30° and 90° using submillisecond kinetic analysis (Yasuda et al., 2001). The 30° substep is attributed to the release of hydrolysis products, and is very similar in magnitude to the rotation of the γ subunit that accompanies the conformational change from the half-closed conformation (β_{ADP+Pi}) to the empty conformation (β_E). The transient intermediate (between the 90° and 30° substeps) observed in the kinetic analysis may therefore be similar to the half-closed conformation in the crystal structure.

While the observed rotation of the γ subunit is consistent with the sense of rotation seen in the direct visualization experiments (Noji et al., 1997), it is possible that the magnitude of the rotation is affected by lattice contacts, as a smaller rotation of 11° is observed in the F_1-DCCD structure (Gibbons et al., 2000) which also has a shrunk unit cell, but has a β_E subunit in the open conformation. However, it is clear from a comparison of the relative positions of the γ and β_E subunits in the native structure and the γ and β_{ADP+Pi} subunits in the $(ADP.AlF_4^-)_2F_1$ structure that some rotation of the γ subunit is essential to accommodate the half-closed conformation of the β_{ADP+Pi} subunit in order to avoid steric clashes between the β and γ subunits. It appears from these structures (and from the native structure where almost half of the γ subunit was disordered) that there is a significant degree of internal flexibility within the γ subunit, which may act as an elastic element coupling the rotation of the ring of c subunits to the conformational changes at the catalytic sites in the intact ATP synthase. This elasticity would be essential if, as suggested from the number of c subunits in the yeast F_1c_{10} subcomplex (Stock et al., 1999), the number of protons translocated per synthesized ATP can be nonintegral.

The Central Stalk

The central stalk in mitochondrial F_1-ATPase is made up of the γ, δ, and ϵ subunits. It provides the structural

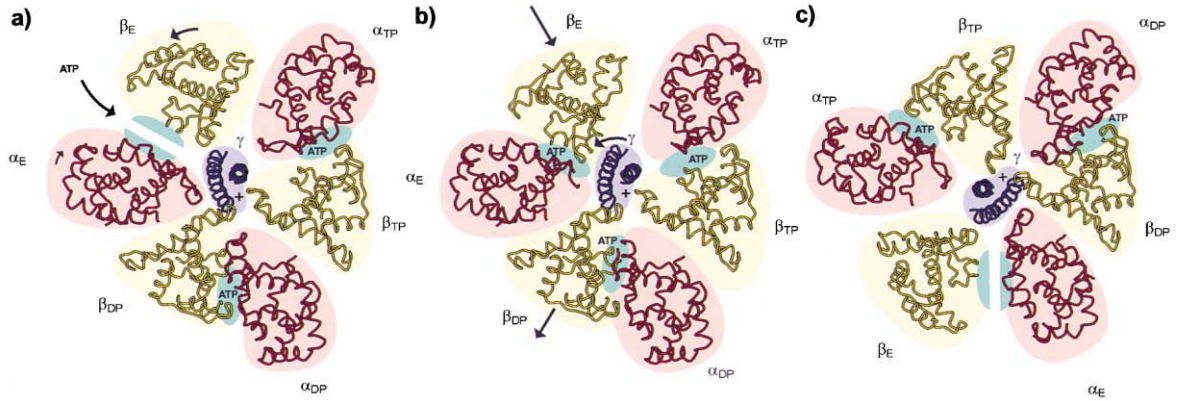

Figure 6. A Model for the Generation of Rotation of the γ Subunit during ATP Hydrolysis in F_1-ATPase

The structures of the C-terminal domains of the α and β subunits are shown in red (pink shading) and yellow (yellow shading), respectively. The coiled-coil region of the γ subunit (residues 3–35 and 221–250) that is in contact with the C-terminal domains is shown in blue (blue shading). The nucleotide binding sites are shown in green. The structure of the native enzyme is shown in (a) and (c), and the $(ADP.AlF_4^-)_2F_1$ structure is shown in (b).

link between the c subunit ring in F_o and the catalytic sites in F_1. Most of the central stalk was disordered in previous F_1-ATPase crystals, but could be modeled in the structure of F_1-ATPase inhibited by DCCD (Gibbons et al., 2000). Using the coordinates of that structure as a guide (Protein Data Bank accession code 1e79), a model was built of most of the central stalk region. However, the electron density is less well defined in the $(ADP.AlF_4^-)_2F_1$ structure and several segments of the γ subunit (residues 58–66, 97–100, 118–126, and 151–156), and the central region of the ϵ subunit (residues 26–36), could not be built. The entire C-terminal helix-turn-helix domain of the δ subunit (residues 104–146) has also been omitted.

The conformation of the γ subunit is very similar in the F_1-DCCD and $(ADP.AlF_4^-)_2F_1$ structures (rmsd 0.69 Å), apart from a difference in the degree of twisting of the coiled-coil region. The β sandwich domain of the δ subunit is essentially identical in both structures (rmsd 0.30 Å). Although the C-terminal helical domain could not be modeled in the $(ADP.AlF_4^-)_2F_1$ structure, a large number of islands of electron density suggest that it packs against the β sandwich domain in a very similar way to that found in the F_1-DCCD structure, rather than adopting the radically different conformation found in the crystal structure of a γ'-ϵ subunit complex of the *E. coli* enzyme (Rodgers and Wilce, 2000). The conformation of the bovine ϵ subunit is also conserved in the two bovine structures (rmsd 0.24 Å). The novel (half-closed) conformation of the β_{ADP+Pi} subunit does not appear to affect either the structures of the individual γ, δ, and ϵ subunits, or the way that they associate to form the central stalk.

Catalytic Cooperativity and the Mechanism of Generation of Rotation in F_1-ATPase

F_1-ATPase (and ATP synthase) display negative cooperativity in substrate binding (typical K_d values are 10^{-12} M, 30 μM, and 150 μM for the bovine enzyme; Cross et al., 1982) and positive cooperativity in catalysis (turnover rates of 10^{-4} s^{-1} for substoichiometric concentrations of ATP increasing to 600 s^{-1} under saturating conditions; Cross et al., 1982). It is now generally accepted that the transition between the different catalytic states of the β subunits is the result of physical rotation of the γ subunit relative to the $(\alpha\beta)_3$ sector, although there is not unanimous agreement (McCarty et al., 2000). On the basis of the structural data currently available, it is possible to propose a model for the generation of rotation (Figure 6). The central feature of this model is a high degree of cooperativity between conformational changes occurring simultaneously in two of the three catalytic β subunits, as in the catalytic scheme proposed by Allison (Ren and Allison, 2000). Commencing with the point at which product (ADP+Pi) has just been released from one of the β subunits (Figure 6a), the next step on the catalytic pathway is the binding of substrate (ATP) to the empty β subunit. The binding energy of ATP is used to generate a conformational change in this subunit, initially from the open conformation (β_E) to a half-closed conformation similar to β_{ADP+Pi}. This partial closure of the β_E subunit produces small conformational changes in the α_E subunit, which are relayed to the catalytic site of the adjacent β_{DP} subunit. This converts the β_{DP} subunit catalytic site to a state committed to ATP hydrolysis (possibly as a result of a shift in the position of α_{DP}Arg373 relative to the bound nucleotide). The energy released by the hydrolysis of ATP on the β_{DP} subunit drives this subunit toward an open conformation, and simultaneously the binding energy of ATP promotes the closure of the β_E subunit. The concerted movement of the C-terminal domains of these two β subunits is responsible for the rotation of the γ subunit; the β_{DP} C-terminal domain moves outwards from the axis of the assembly, while that of the β_E subunit moves in toward this axis (Figures 6b and 6c). Van der Waal's interactions between residues in these C-terminal domains (β385–395) and the γ subunit (γ12–19, γ25–30, and γ234–242) are primarily responsible for the movement of the γ subunit. The cooperativity between the catalytic sites arises because γ subunit rotation is dependent upon conformational changes in both β subunits; neither ATP hydro-

lysis alone nor ATP binding alone is sufficient to generate the rotation. Comparison of the closed and half-closed conformations of the β subunit reveals a possible mechanism for the observed domain rotation. Hydrolysis of ATP results in a 3.5–4 Å movement of the cleaved γ-phosphate (modeled by the sulfate), presumably driven by electrostatic repulsion between the β- and γ-phosphate groups. The shift in the γ-phosphate is accommodated by the movement of βTyr311, which forms the "top" of the nucleotide binding pocket (Figure 2a). This tyrosine residue lies at the C-terminal end of β strand 7 in the nucleotide binding domain, and its movement results in the separation of this strand from the C-terminal end of the adjacent β strand 3, with the loss of 2–3 interstrand hydrogen bonds (Figures 3c and 3d). The separation of these two β strands generates the rotation of the lower three strands of the β sheet, together with the C-terminal domain, relative to the upper part of the nucleotide binding domain.

The proposed scheme is consistent with the direction of rotation observed in the direct visualization experiments (Noji et al., 1997). The concerted nature of the conformational changes in the two β subunits also implies that at no stage in the catalytic cycle does the enzyme adopt a symmetric state. This is entirely consistent with the inherent asymmetry in subunit stoichiometry and with the observed asymmetric location of the γ subunit within the $(\alpha\beta)_3$ assembly.

Experimental Procedures

Purification, Crystallization, and Data Collection

Bovine F_1-ATPase was purified as described previously (Lutter et al., 1993) but without stripping of endogenous nucleotide. The enzyme was then exchanged into a buffer containing 5 mM Tris/SO_4 (pH 8.0) and 20% (v/v) glycerol using a NaP 10 desalting column (Pharmacia Biotech, St. Albans, Herts., United Kingdom) and inhibited with aluminium fluoride as described previously (Braig et al., 2000). Crystals of the inhibited F_1-ATPase were grown by microdialysis using previously published conditions (Lutter et al., 1993), except that both inside and outside buffers were free of AMPPNP and contained 660 μM ADP, 1 mM $AlCl_3$, and 5 mM NaF. Crystals with typical dimensions of 0.3 × 0.2 × 0.15 mm grew over a period of 4–6 weeks. After harvesting into a buffer containing 13% PEG 6000, the glycerol concentration was increased stepwise to 5%, 10%, 15%, and 20% (2 hr at each concentration) immediately before data collection. Diffraction data were collected from a single cryocooled crystal (100 K) using an ADSC Quantum Four CCD detector on beamline 9.6 at the SRS, Daresbury, United Kingdom (λ = 0.87 Å). Crystals belong to the spacegroup $P2_12_12_1$ with unit cell dimensions a = 267.7 Å, b = 106.2 Å, c = 138.3 Å. The diffraction data were integrated with MOSFLM (Leslie, 1992) and processed further with programs from the Collaborative Computational Project Number 4 (CCP4) suite (Collaborative Computational Project Number 4, 1994).

Structure Solution and Refinement

The structure was solved by molecular replacement with AmoRe (Navaza, 1994) using the native F_1-ATPase structure (Protein Data Bank accession code 1bmf) as search model. Following rigid body refinement with AmoRe, the final R factor and correlation coefficient were 37.2% and 61.3%, respectively, for all data between 13.5 Å and 4.0 Å resolution. Further rigid body refinement was carried out with TNT (Tronrud et al., 1987), followed by alternating rounds of manual rebuilding using O (Jones et al., 1991) and positional refinement with REFMAC (Murshudov et al., 1997) using all data from 13.5–2.0 Å resolution. MgADP.AlF_4^- was modeled in the β_{TP} and β_{DP} subunits and MgADP was modeled in the β_E subunit. Well-defined electron density for a tetrahedral group close to the β-phosphate of ADP in the β_E subunit (Figure 1) was modeled as a sulfate ion (20 mM $MgSO_4$ was present in the crystallization medium). The final model includes four glycerol and 1693 water molecules (Table 1). The stereochemistry was assessed with PROCHECK (Laskowski et al., 1993), which assigned 89.7% of the residues to the most favored region of the Ramachandran plot, 9.7% to additional allowed regions, and 0.6% to generously allowed regions. There are no residues in disallowed regions.

Structure comparisons and the determination of rotation axis parameters were performed with the CCP4 program SUPERPOSE. Figures 1, 2a, 3, and 5 were prepared using BOBSCRIPT (Esnouf, 1997).

Acknowledgments

We thank Dr. Daniela Stock for help with data collection, staff at the SRS, Daresbury, UK for support, and Dr. P.R. Evans for comments on the manuscript. R.I.M. was the recipient of a Fellowship from the Human Frontier Science Program.

Received January 19, 2001; revised June 29, 2001.

References

Abrahams, J.P., Leslie, A.G.W., Lutter, R., and Walker, J.E. (1994). Structure at 2.8 Å resolution of F_1-ATPase from bovine heart mitochondria. Nature *370*, 621–628.

Amano, T., Tozawa, K., Yoshida, M., and Murakami, H. (1994). Spatial precision of a catalytic carboxylate of F_1-ATPase Beta-subunit probed by introducing different carboxylate-containing side-chains. FEBS Lett. *348*, 93–98.

Amano, T., Hisabori, T., Muneyuki, E., and Yoshida, M. (1996). Catalytic activities of $\alpha3\beta3\gamma$ complexes of F_1-ATPase with 1, 2, or 3 incompetent catalytic sites. J. Biol. Chem. *271*, 18128–18133.

Boyer, P.D. (1993). The binding change mechanism for ATP synthase—some probabilities and possibilities. Biochim. Biophys. Acta *1140*, 215–250.

Boyer, P.D. (1997). The ATP synthase—a splendid molecular machine. Annu. Rev. Biochem. *66*, 717–749.

Boyer, P.D. (2000). Catalytic site forms and controls in ATP synthase catalysis. Biochim. Biophys. Acta *1458*, 252–262.

Braig, K., Menz, R.I., Montgomery, M.G., Leslie, A.G.W., and Walker, J.E. (2000). Structure of bovine mitochondrial F_1-ATPase inhibited by Mg^{2+} ADP and aluminium fluoride. Structure *8*, 567–573.

Collaborative Computational Project Number 4 (1994). The CCP4 Suite: Programs for Protein Crystallography. Acta Crystallogr. D Biol. Crystallogr. *50*, 760–763.

Cross, R.L., Grubmeyer, C., and Penefsky, H.S. (1982). Mechanism of ATP hydrolysis by beef heart mitochondrial ATPase. Rate enhancements resulting from cooperative interactions between multiple catalytic sites. J. Biol. Chem. *257*, 12101–12105.

Deckers-Hebestreit, G., and Altendorf, K. (1996). The F_0F_1-type ATP synthases of bacteria: structure and function of the F_o complex. Annu. Rev. Microbiol. *50*, 791–824.

Dou, C., Grodsky, N.B., Matsui, T., Yoshida, M., and Allison, W.S. (1997). ADP-fluoroaluminate complexes are formed cooperatively at two catalytic sites of wild-type and mutant $\alpha3\beta3\gamma$ subcomplexes of the F_1ATPase from the thermophilic *Bacillus* PS3. Biochemistry *36*, 3719–3727.

Duncan, T.M., Bulygin, V.V., Zhou, Y., Hutcheon, M.L., and Cross, R.L. (1995). Rotation of subunits during catalysis by *Escherichia coli* F_1-ATPase. Proc. Natl. Acad. Sci. USA *92*, 10964–10968.

El-Shawi, M.K., Parsonage, D., and Senior, A.E. (1990). Thermodynamic analyses of the catalytic pathway of F_1-ATPase from *Escherichia coli*—implications regarding the nature of energy coupling by F_1-ATPases. J. Biol. Chem. *265*, 4402–4410.

Esnouf, R.M. (1997). An extensively modified version of MolScript that includes greatly enhanced coloring capabilities. J. Mol. Graph. Model. *15*, 132–134.

Feldman, R.I., and Sigman, D.S. (1983). The synthesis of ATP by the

membrane-bound ATP synthase complex from medium ^{32}Pi under completely uncoupled conditions. J. Biol. Chem. *258*, 12178–12183.

Fersht, A. (1998). Structure and Mechanism in Protein Science (New York: W.H. Freeman).

Gibbons, C., Montgomery, M.G., Leslie, A.G.W., and Walker, J.E. (2000). The structure of the central stalk in bovine F_1-ATPase at 2.4 A resolution. Nat. Struct. Biol. *7*, 1055–1061.

Issartel, J.P., Dupuis, A., Lunardi, J., and Vignais, P.V. (1991). Fluoroaluminum and fluoroberyllium nucleoside diphosphate complexes as probes of the enzymatic mechanism of the mitochondrial F_1-ATPase. Biochemistry *30*, 4726–4733.

Jones, T.A., Zou, J.Y., Cowan, S.W., and Kjeldgaard (1991). Improved methods for binding protein models in electron density maps and the location of errors in these models. Acta Crystallogr. A *47*, 110–119.

Laskowski, R.A., MacArthur, M.W., Moss, D.S., and Thornton, J.M. (1993). PROCHECK—a program to check the stereochemical quality of protein structures. J. Appl. Cryst. *26*, 283–291.

Le, N.P., Omote, H., Wada, Y., AlShawi, M.K., Nakamoto, R.K., and Futai, M. (2000). *Escherichia coli* ATP synthase alpha subunit Arg-376: The catalytic site arginine does not participate in the hydrolysis/synthesis reaction but is required for promotion to the steady state. Biochemistry *39*, 2778–2783.

Leslie, A.G.W. (1992). Joint CCP4 and EACMB Newsletter Protein Crystallography (Warrington, United Kingdom: Daresbury Laboratory).

Lobau, S., Weber, J., WilkeMounts, S., and Senior, A.E. (1997). F_1-ATPase, roles of three catalytic site residues. J. Biol. Chem. *272*, 3648–3656.

Lutter, R., Abrahams, J.P., Van Raaij, M.J., Todd, R.J., Lundqvist, T., Buchanan, S.K., Leslie, A.G.W., and Walker, J.E. (1993). Crystallisation of F_1-ATPase from bovine heart mitochondria. J. Mol. Biol. *229*, 787–790.

Masaike, T., Mitome, N., Noji, H., Muneyuki, E., Yasuda, R., Kinosita, K., and Yoshida, M. (2000). Rotation of F_1-ATPase and the hinge residues of the beta subunit. J. Exp. Biol. *203*, 1–8.

McCarty, R.E., Evron, Y., and Johnson, E.A. (2000). The chloroplast ATP synthase: A rotary enzyme? Annu. Rev. Plant Physiol. Plant Mol. Biol. *51*, 83–109.

Murshudov, G.N., Vagin, A.A., and Dodson, E.J. (1997). Refinement of macromolecular structures by the maximum-likelihood method. Acta Crystallogr. D Biol. Crystallogr. *53*, 240–255.

Nadanaciva, S., Weber, J., and Senior, A.E. (1999a). The role of βArg-182, an essential catalytic site residue in *Escherichia coli* F_1-ATPase. Biochemistry *38*, 7670–7677.

Nadanaciva, S., Weber, J., WilkeMounts, S., and Senior, A.E. (1999b). Importance of F_1-ATPase residue αArg-376 for catalytic transition state stabilization. Biochemistry *38*, 15493–15499.

Nadanaciva, S., Weber, J., and Senior, A.E. (2000). New probes of the F_1-ATPase catalytic transition state reveal that two of the three catalytic sites can assume a transition state conformation simultaneously. Biochemistry *39*, 9583–9590.

Navaza, J. (1994). AMoRe: an automated package for molecular replacement. Acta Crystallogr. A *50*, 157–163.

Noji, H., Yasuda, R., Yoshida, M., and Kinosita, K. (1997). Direct observation of the rotation of F_1-ATPase. Nature *386*, 299–302.

Ren, H., and Allison, W.S. (2000). On what makes the γ-subunit spin during ATP hydrolysis by F_1. Biochim. Biophys. Acta *1458*, 221–233.

Rodgers, A.J., and Wilce, M.C. (2000). Structure of the gamma-epsilon complex of ATP synthase. Nat. Struct. Biol. *7*, 1051–1054.

Rosing, J., Kayalar, C., and Boyer, P.D. (1977). Evidence for energy-dependent change in phosphate binding for mitochondrial oxidative phosphorylation based on measurements of medium and intermediate phosphate-water exchanges. J. Biol. Chem. *252*, 2478–2485.

Sabbert, D., Engelbrecht, S., and Junge, W. (1996). Intersubunit rotation in active F-ATPase. Nature *381*, 623–625.

Stock, D., Leslie, A.G.W., and Walker, J.E. (1999). Molecular architecture of the rotary motor in ATP synthase. Science *286*, 1700–1705.

Stryer, L. (1995). Biochemistry (New York: W.H. Freeman).

Tronrud, D.E., Ten Eyck, L.F., and Matthews, B.W. (1987). An efficient general-purpose least-squares refinement program for macromolecular structures. Acta Crystallogr. A *43*, 489–501.

Tsunoda, S.P., Muneyuki, E., Amano, T., Yoshida, M., and Noji, H. (1999). Cross-linking of two beta subunits in the closed conformation in F1-ATPase. J. Biol. Chem. *274*, 5701–5706.

Walker, J.E. (1998). ATP synthesis by rotary catalysis (Nobel Lecture). Angew. Chem. Int. Ed. Engl. *37*, 2309–2319.

Weber, J., and Senior, A.E. (1997). Catalytic mechanism of F_1-ATPase. Biochim. Biophys. Acta *1319*, 19–58.

Weber, J., and Senior, A.E. (2000). ATP synthase: what we know about ATP hydrolysis and what we do not know about ATP synthesis. Biochim. Biophys. Acta *1458*, 300–309.

Weber, J., Bowman, C., and Senior, A.E. (1996). Specific tryptophan substitution in catalytic sites of *Escherichia coli* F_1-ATPase allows differentiation between bound substrate ATP and product ADP in steady-state catalysis. J. Biol. Chem. *271*, 18711–18718.

Weber, J., Wilke-Mounts, S., Lee, R.S.F., Grell, E., and Senior, A.E. (1993). Specific placement of tryptophan in the catalytic sites of *Escherichia-coli* F_1-ATPase provides a direct probe of nucleotide-binding—maximal ATP hydrolysis occurs with 3 sites occupied. J. Biol. Chem. *268*, 20126–20133.

Yasuda, R., Noji, H., Yoshida, M., Kinosita, K., Jr., and Itoh, H. (2001). Resolution of distinct rotational substeps by submillisecond kinetic analysis of F1-ATPase. Nature *410*, 898–904.

Accession Numbers

The structure reported in this paper has been deposited in the Protein Data Bank under ID code 1H8E.